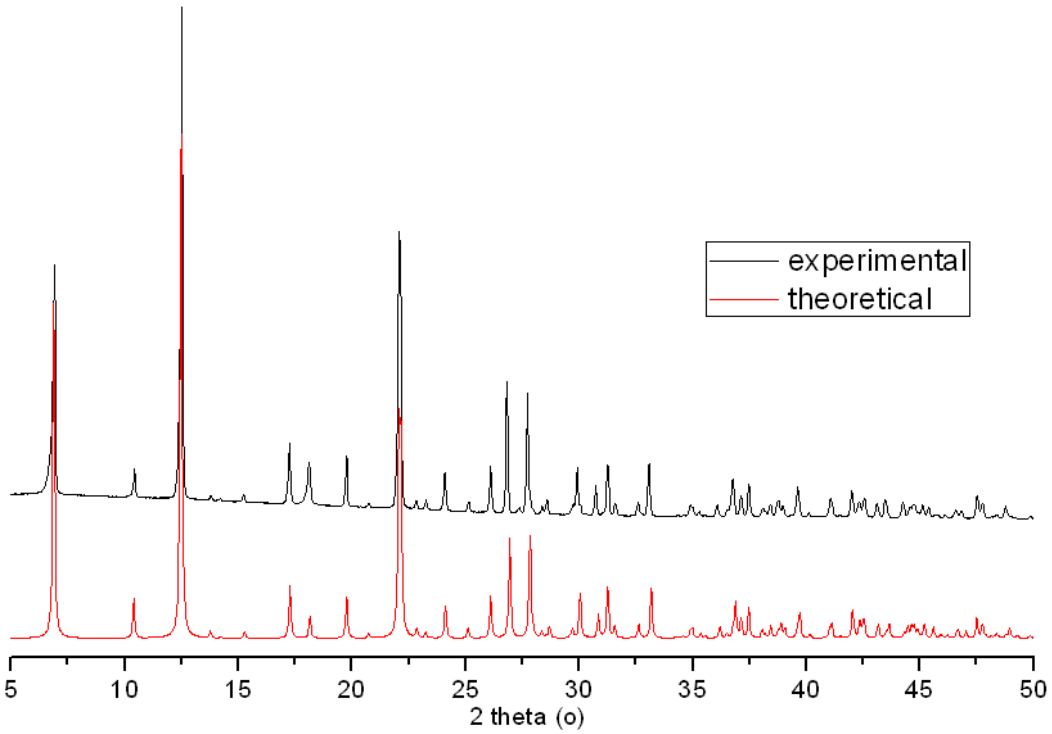

Fig. S1 The powder XRD pattern of compound **3** (experimental) and the simulation of the powder pattern of **3** from the crystal structure.

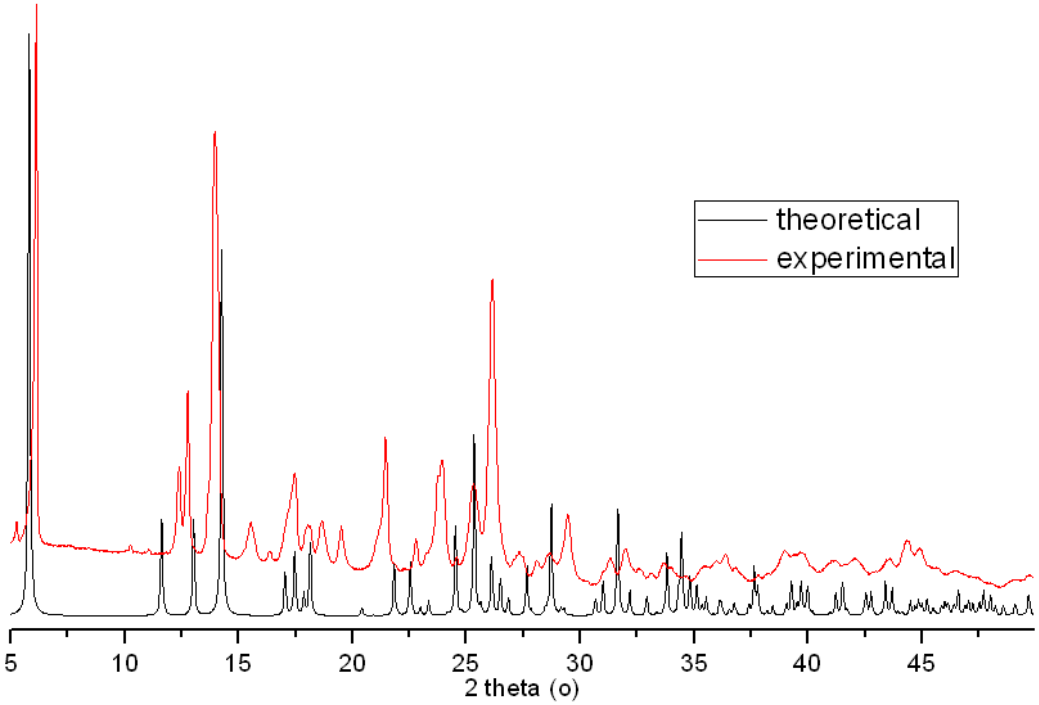

Fig. S2 The powder XRD pattern of compound **4** (experimental) and the simulation of the powder pattern of **4** from the crystal structure.

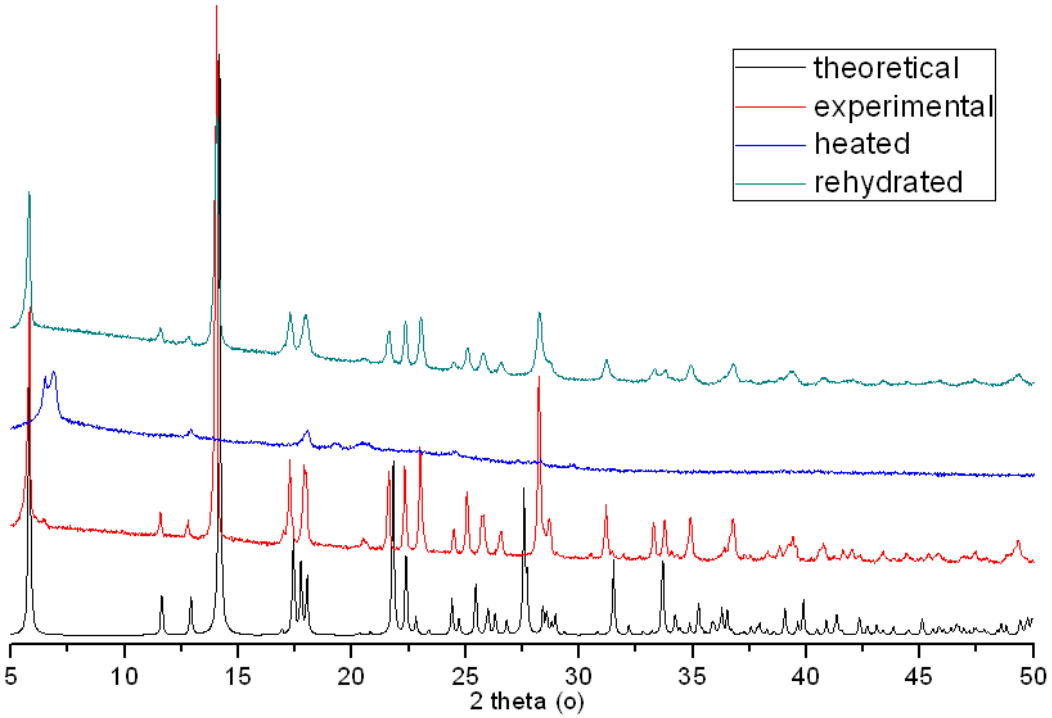

Fig. S3 The powder XRD pattern of compound **6** (experimental), the rehydrated analogue of **6** and the simulation of the powder pattern of **6** from the crystal structure.

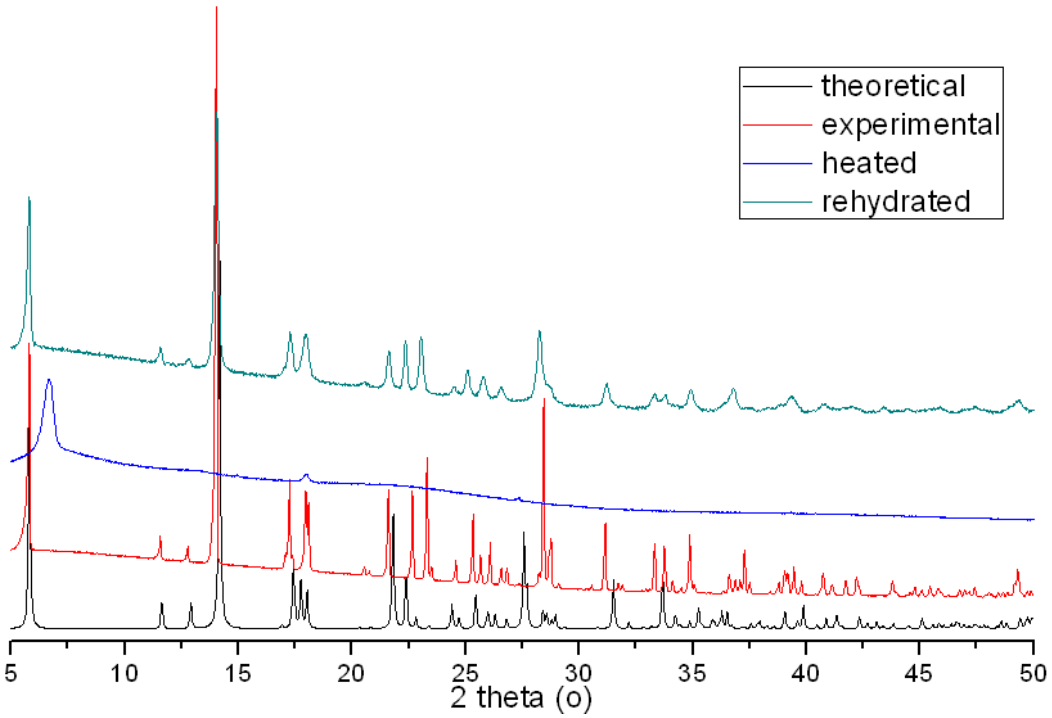

Fig. S4 The powder XRD pattern of compound **7** (experimental), the rehydrated analogue of **7** and the simulation of the powder pattern of **7** from the crystal structure.

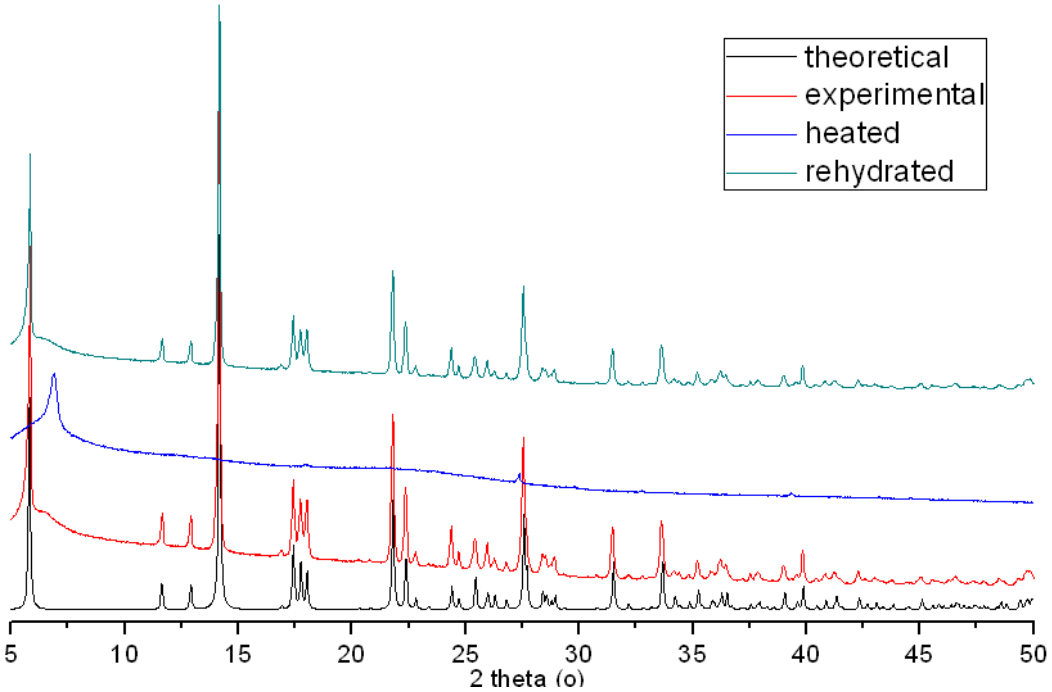

Fig. S5 The powder XRD pattern of compound **8** (experimental), the rehydrated analogue of **8** and the simulation of the powder pattern of **8** from the crystal structure.

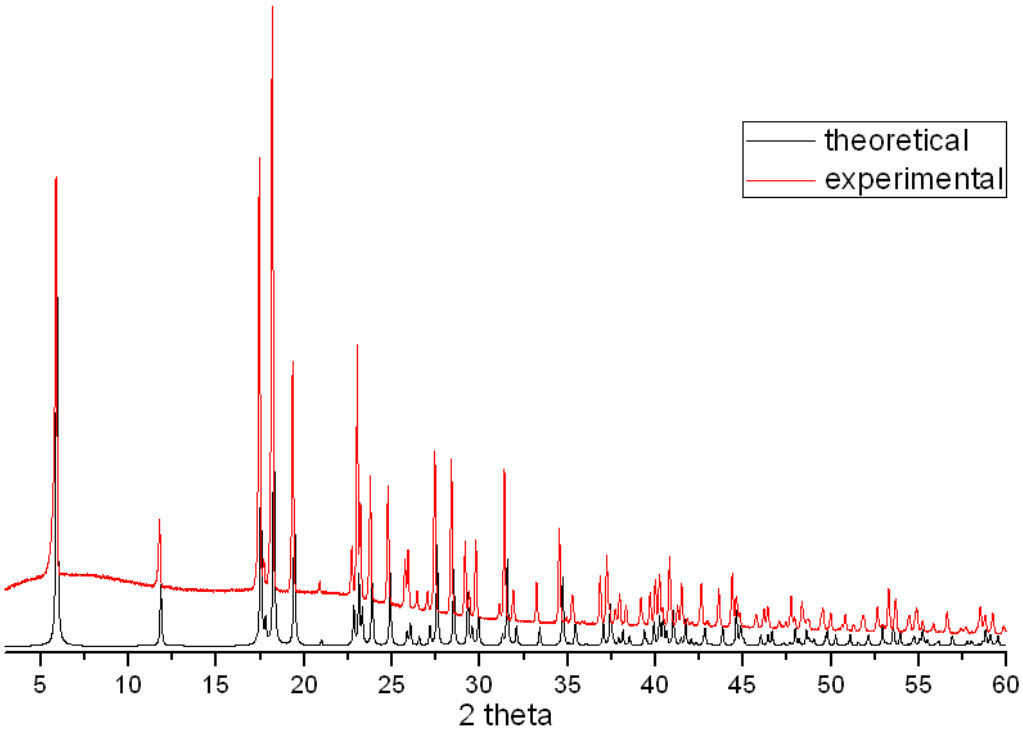

Fig. S6 The powder XRD pattern of compound **9** (experimental) and the simulation of the powder pattern of **9** from the crystal structure

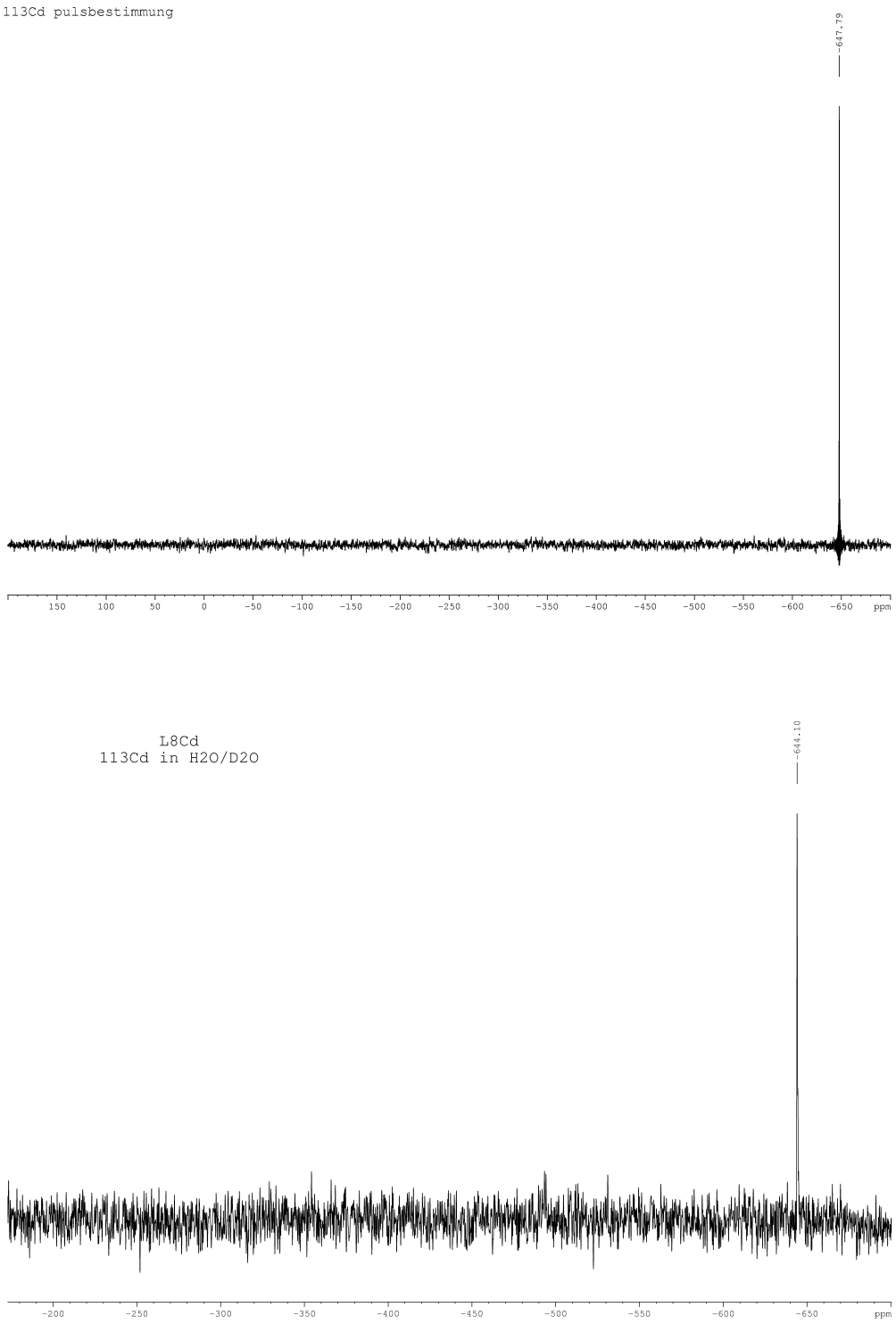

Fig. S7. (up) ^{113}Cd NMR spectra of the reference and (down) 113CdNMR spectra of compound **9**.

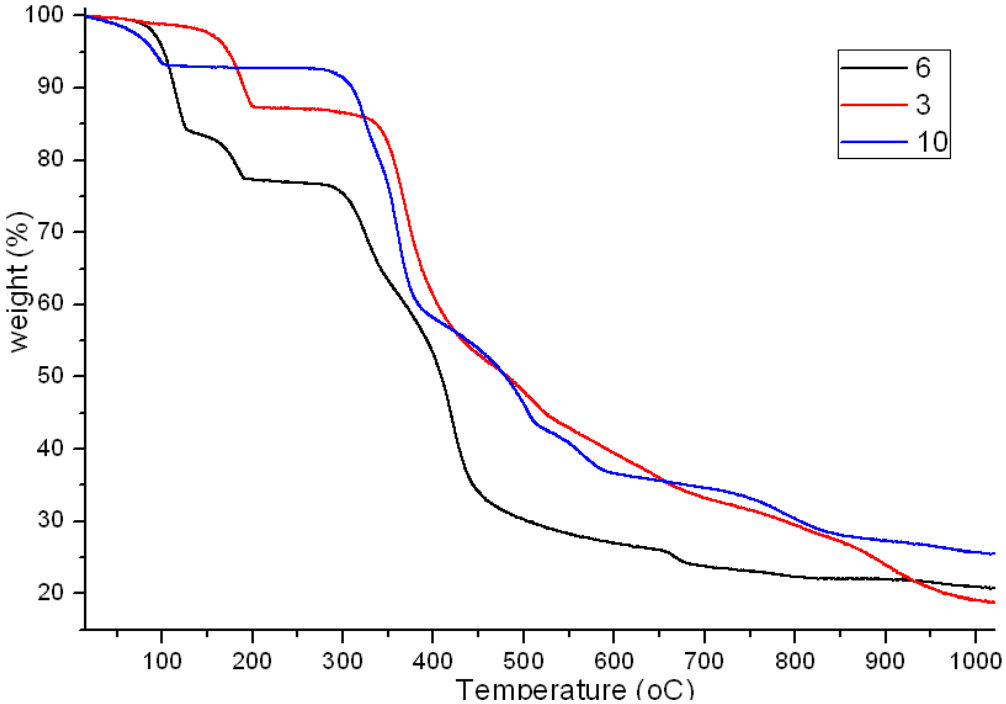

Fig. S8 TGA curves for compounds **3, 6** and **10**.

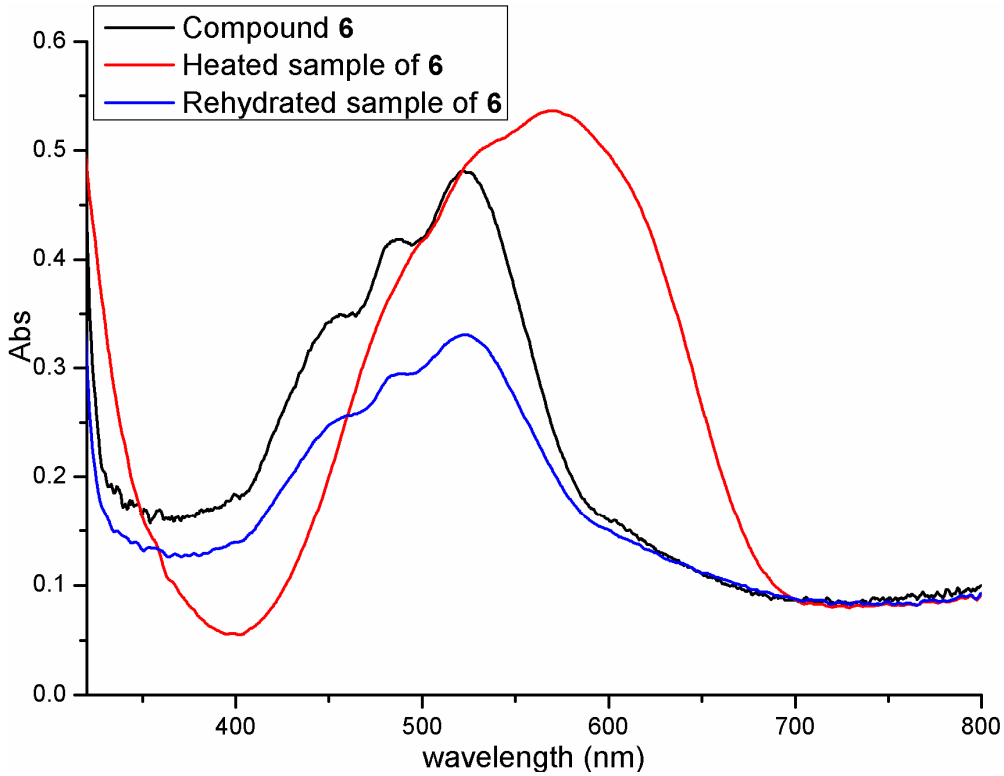

Fig. S9 DRS spectra for compound **6**

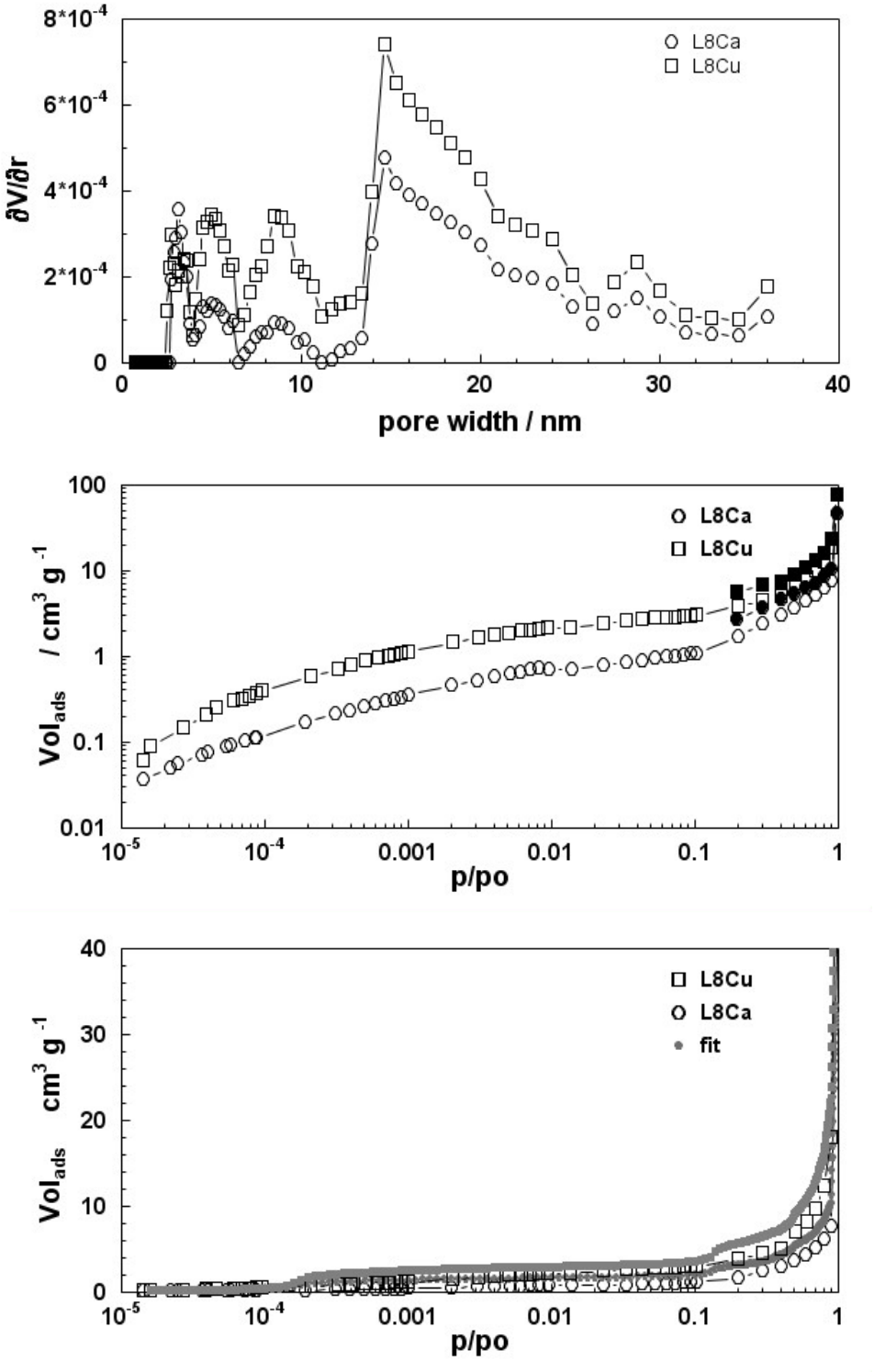

Fig. S10 (upper) Pore width distribution (middle) Isotherm vs partial pressure (lower) Isotherms Fitting

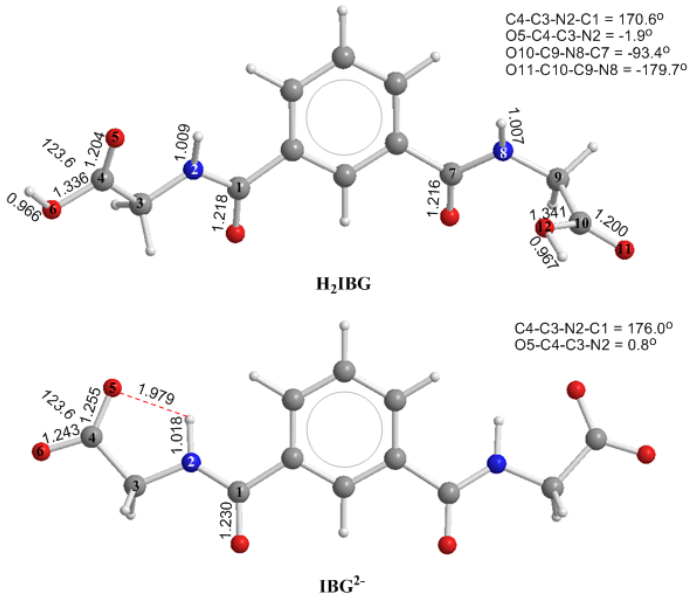

Fig. S11 Equilibrium geometries of the free-standing" H_2IBG (**1**) ligand and its deprotonated dianionic conjugate base IBG^{2-} calculated at the PBE0/6-311+G(d,p) level.

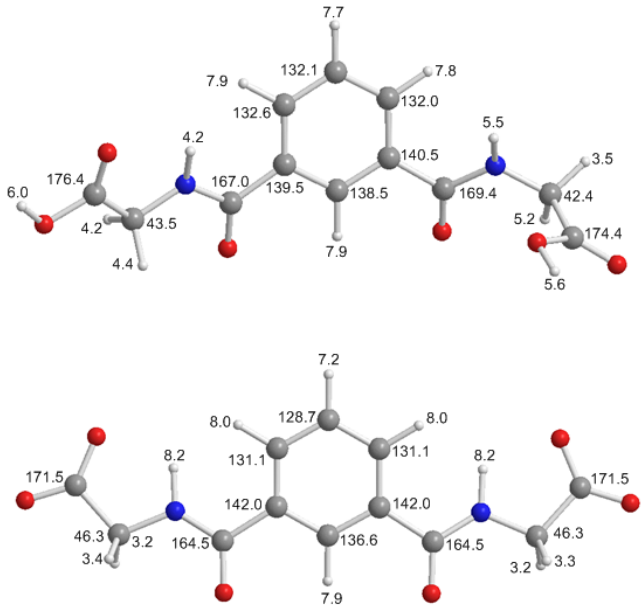

Fig. S12 ^{1}H and ^{13}C NMR chemical shifts (δ, ppm) of the free-standing" H_2IBG and IBG^{2-} species calculated at the GIAO-PBE0/6-311+G(d,p) level.

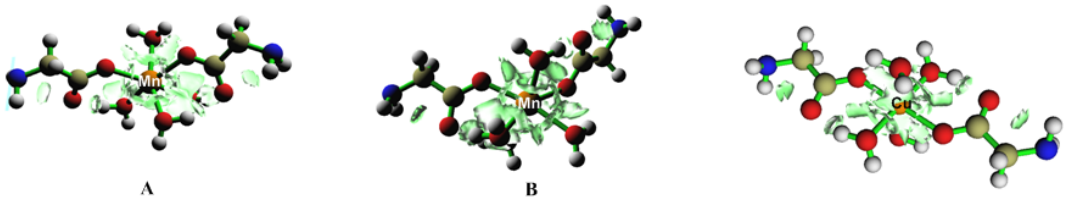

Fig. S13 3D plots of the Reduced Density Gradient (RDG) (isosurface = 0.700) for the $Mn(glycine)_2(H_2O)_4$ and $Cu(glycine)_2(H_2O)_4$ complexes calculated at the DSD-PBEP86/Def2-TZVP level